

## The sintering temperature effects on the electrical and dielectric properties of Li 0.05 Ti 0.02 Ni 0.93 O ceramics prepared by a direct thermal decomposition method

Prasit Thongbai, Teerapon Yamwong, and Santi Maensiri

Citation: [Journal of Applied Physics](#) **104**, 074109 (2008); doi: 10.1063/1.2990768

View online: <http://dx.doi.org/10.1063/1.2990768>

View Table of Contents: <http://scitation.aip.org/content/aip/journal/jap/104/7?ver=pdfcov>

Published by the [AIP Publishing](#)

---

### Articles you may be interested in

[Low dielectric loss, dielectric response, and conduction behavior in Na-doped Y2/3Cu3Ti4O12 ceramics](#)  
J. Appl. Phys. **116**, 044101 (2014); 10.1063/1.4891240

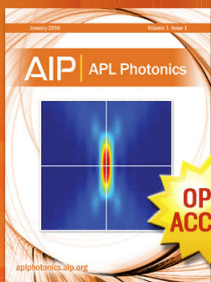
[Origin of giant permittivity and high-temperature dielectric anomaly behavior in Na0.5Y0.5Cu3Ti4O12 ceramics](#)  
J. Appl. Phys. **113**, 224102 (2013); 10.1063/1.4809927

[Intrinsic and extrinsic relaxation of CaCu 3 Ti 4 O 12 ceramics: Effect of sintering](#)  
J. Appl. Phys. **108**, 104104 (2010); 10.1063/1.3511444

[Electric and dielectric properties of Bi-doped CaCu 3 Ti 4 O 12 ceramics](#)  
J. Appl. Phys. **105**, 076104 (2009); 10.1063/1.3106054

[Effects of Fe, Ti, and V doping on the microstructure and electrical properties of grain and grain boundary of giant dielectric NiO-based ceramics](#)  
Appl. Phys. Lett. **94**, 022908 (2009); 10.1063/1.3072356

---



Launching in 2016!  
The future of applied photonics research is here

AIP | APL  
Photonics

# The sintering temperature effects on the electrical and dielectric properties of $\text{Li}_{0.05}\text{Ti}_{0.02}\text{Ni}_{0.93}\text{O}$ ceramics prepared by a direct thermal decomposition method

Prasit Thongbai,<sup>1</sup> Teerapon Yamwong,<sup>2</sup> and Santi Maensiri<sup>1,a)</sup>

<sup>1</sup>Department of Physics, Khon Kaen University, Khon Kaen 40002, Thailand

<sup>2</sup>National Metals and Materials Technology Center (MTEC), Thailand Science Park, Pathumthani 12120, Thailand

(Received 10 June 2008; accepted 12 August 2008; published online 7 October 2008)

We reported the effects of grain size on high dielectric and related electrical properties of  $\text{Li}_{0.05}\text{Ti}_{0.02}\text{Ni}_{0.93}\text{O}$  (LTNO) ceramics, which were prepared by a direct thermal decomposition method. The analysis of complex impedance indicated that these LTNO ceramics were electrically heterogeneous consisting of conducting grains and insulating grain boundaries (GBs). Interestingly, our results revealed that the dielectric permittivity ( $\epsilon'$ ) increases with the increase in grain size, which can be well described by Maxwell–Wagner relaxation model. Furthermore, we also found that the activation energy required for relaxation process ( $E_a$ ) and related activation energy of the conductivity in the grain interior ( $E_g$ ) decreased with the increase in grain size. These results suggested that the different microstructures resulted in chemical change (e.g., oxygen vacancies) inside the grains, leading to the changes in electrical properties of the LTNO ceramics. © 2008 American Institute of Physics. [DOI: 10.1063/1.2990768]

## I. INTRODUCTION

Dielectric oxide ceramics with high dielectric permittivity ( $\epsilon'$ ) have raised considerable research attentions in recent years because these oxides play an important role in microelectronics and have numerous technological applications such as capacitors and memory devices.<sup>1</sup> Generally, high-permittivity dielectric materials are ferroelectric and relaxor oxides. However, both kinds of materials have  $\epsilon'$  values that strongly depend on temperature and their structures contain lead, which pollutes the environment. Therefore, lead-free materials with high- $\epsilon'$  and good thermal stability are becoming increasingly attractive. These promising materials recently reported include  $\text{CaCu}_3\text{Ti}_4\text{O}_{12}$  (CCTO),<sup>1–9</sup> ( $M,N$ )-doped NiO systems ( $M=\text{Li, Na, K}$  and  $N=\text{Ti, Al, Si, Ta}$ ),<sup>10–16</sup> and  $\text{CuO}$ .<sup>17,18</sup> Most of the researchers attribute such a high apparent  $\epsilon'$  to Maxwell–Wagner (MW) relaxation as a result of semiconducting properties inside grains and insulating properties at grain boundary (GB) (Ref. 6) or electrode interfaces.<sup>9</sup>

For nonperovskite ( $M, N$ )-doped NiO materials, it is now widely accepted that the high- $\epsilon'$  at radio frequencies is associated with internal barrier layer capacitance (IBLC) effect arising from core/shell structure, which induces MW polarization (i.e., interfacial polarization) at the interfaces between grains and GBs.<sup>19</sup> The  $N$ -dopant is rich on the GBs (indigent within the grains) and forms a second phase, which acts as an insulator enclosing the core of the grain which is semiconductive  $M$ -doped NiO particles, and the polarization relaxation is closely related with the conductivity in the grain interior.<sup>19</sup> Moreover, Lin *et al.*<sup>20</sup> have found that the huge- $\epsilon'$  response of  $\text{Li}_x\text{Ti}_y\text{Ni}_{1-x-y}\text{O}$  system could be also enhanced

by the polarization of defect dipoles such as oxygen vacancies. Normally, such defect is easily induced by processing conditions (e.g., sintering temperature and duration of sintering),<sup>6,21–24</sup> and the concentration of defect depend on the microstructure of ceramics such as grain size.<sup>25</sup> Therefore, the processing conditions should have a strong influence on the polycrystalline ceramics properties (e.g., electric conductivity and optical and dielectric properties). For examples, the  $\epsilon'$  values of CCTO ceramics increase from 9000 to 280 000 with increasing the sintering time from 3 to 24 h (grain size increases from  $\sim 5$  to  $\sim 100$   $\mu\text{m}$ ) at 1100 °C.<sup>26</sup> Moreover, Shao *et al.*<sup>27</sup> showed that the  $\epsilon'$  values of CCTO ceramics also increase from 1200 to 60 000 with increasing the sintering temperature from 1000 to 1120 °C for 10 h.

Unfortunately, only a few studies have focused on the effect of sintering conditions on the dielectric properties of NiO-based ceramics. The study of the influence of sintering conditions (effects of grain size) on the electrical properties of (Li, Ti)-doped NiO ceramics have not been reported. Generally, the sintering conditions are often used to tune the microstructure of ceramics, leading to dramatic changes in its electrical properties. Thus, investigation of the effects of sintering conditions may not only be useful to optimize the preparing conditions for the future applications, but also be able to provide the important clues about the underlying mechanism governing the intriguing dielectric behavior of ceramics.

In this paper, we report the effects of grain size on dielectric and electrical properties of high- $\epsilon'$   $\text{Li}_{0.05}\text{Ti}_{0.02}\text{Ni}_{0.93}\text{O}$  (LTNO) ceramics synthesized by a simple thermal decomposition method. Our results revealed that high- $\epsilon'$  increased with an increase in grain size. Impedance spectroscopy (IS) indicated that our LTNO ceramics had an electrically heterogeneous structure. The high- $\epsilon'$  behavior and dielectric relax-

<sup>a)</sup>Electronic addresses: sanmae@kku.ac.th and santimaensiri@gmail.com.

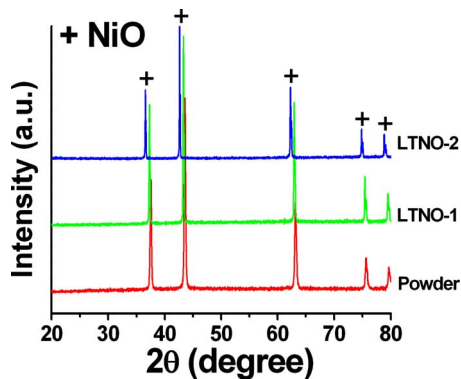


FIG. 1. (Color online) XRD patterns of the LTNO powder and LTNO ceramics (LTNO-1 and LTNO-2).

ation of the LTNO ceramics were also investigated, and it was suggested that such a high- $\epsilon'$  response could be enhanced by the IBLC mechanism through MW relaxation. Interestingly, the activation energy required for relaxation and related conduction activation energy inside the grain decreased with grain size increasing, which was attributed to the effect of oxygen vacancies in ceramics.

## II. EXPERIMENTS

$(\text{CH}_3\text{COO})_2\text{Ni} \cdot 4\text{H}_2\text{O}$  (99.0%, UNILAB),  $\text{C}_2\text{H}_3\text{LiO}_2 \cdot 2\text{H}_2\text{O}$  ( $\geq 97.0\%$ , Fluka), and titanium(diisopropoxide) bis(2,4-pentanedionate) 75 wt % in 2-propanol (Ti-solution) (99%, Acros) were employed as starting raw materials. The polycrystalline LTNO ceramic samples were simply prepared by the following procedure. First, stoichiometric amounts of  $(\text{CH}_3\text{COO})_2\text{Ni} \cdot 4\text{H}_2\text{O}$ ,  $\text{C}_2\text{H}_3\text{LiO}_2 \cdot 2\text{H}_2\text{O}$ , and Ti-solution were dissolved in distilled water and mixed in alumina crucible using a magnetic stirrer. Then, the mixed powder was decomposed at a temperature of 650 °C for 10 h. The obtained LTNO powder was pressed into pellets of 9.5 mm in diameter and  $\sim 1$ –2 mm in thickness by a uniaxial pressing method at 200 MPa. Finally, these pellets were sintered at 1200 and 1280 °C for 4 h in air. Throughout this paper, we assigned symbols of LTNO-1 and LTNO-2 for the samples sintered at 1200 and 1280 °C, respectively.

The sintered ceramics were characterized by x-ray diffraction (XRD) (Philips PW3040, The Netherlands) and scanning electron microscopy (SEM) (Hitachi S-4700, Japan). The ceramic samples were polished and electroded by silver paint on both sides of the disk-shaped samples. They were allowed to dry overnight. The dielectric response of the samples was measured using a Hewlett Packard 4194 A impedance gain phase analyzer over the frequency ranging from 100 Hz to 10 MHz and at the oscillation voltage of 1.0 V. The measurements were performed over the temperature

ranging from  $-50$  to  $130$  °C using an inbuilt cooling-heating system. Each measured temperature was kept constant with an accuracy of  $\pm 1$  °C.

## III. RESULTS AND DISCUSSION

Figure 1 displays the XRD patterns of the prepared LTNO powder and sintered ceramics with different sintering temperatures, confirming a single phase of NiO in the powder and ceramic samples. We have thus produced good LTNO powder at a much lower reaction temperature compared to those prepared by conventional sol-gel route<sup>10</sup> and polymerized complex route.<sup>11</sup> All of the main peaks are comparable to that of powder diffraction pattern of NiO in Ref. 32. The values of lattice parameter calculated from XRD spectra are shown in Table I. These values are close to value reported in Ref. 32. Additionally, it is also important to notice that a normal insulating phase  $\text{NiTiO}_3$  was not detected in the XRD patterns. This is not surprising given that the typical detection limit of the technique when the Ti content is less than 0.05 and/or it might be attributed to the Ti-dopant content, which is not over the solid solution limitation of Ti–Ni–O system, forming a single solid solution.

The surface morphology of LTNO samples was revealed by SEM, as shown in Figs. 2(a) and 2(b). It is clear that the grain size increases with increasing the sintering temperature. The mean grain sizes are about  $2.67 \pm 0.75$  and  $6.02 \pm 2.38$   $\mu\text{m}$  for LTNO-1 and LTNO-2 samples. Note that large portion of porosity is observed in the microstructure of LTNO-1 sample, but LTNO-2 sample is dense ceramic.

To confirm the existence of electrically inhomogeneous in our LTNO samples, IS, which is a powerful tool in separating out the bulk and the GBs effects,<sup>28</sup> was carried out. In general, Fig. 3(a) shows the impedance spectra of LTNO-2 sample as a function of temperature. The impedance semicircles became larger with decreasing temperature. When the temperature was sufficiently low, other impedance semicircles were observed [inset of Fig. 3(a)]. Note that the LTNO-1 sample also shows a similar spectra (not present). The observation of two semicircles suggests that our LTNO ceramics are electrically heterogeneous and the core/shell model could be appropriated for further analysis. These results are similar to the other report in literature.<sup>19</sup> Accordingly, the observed semicircles at high and low temperatures can be assigned to the effect of charge transport within the grain and GB, respectively. The charge transport inside the grain is mainly affected by the addition of Li ions in NiO, leading to an increase of conductivity and some defects can be introduced due to different valences of doped ions ( $0.69$  Å for  $\text{Ni}^{2+}$  and  $0.68$  Å for  $\text{Li}^+$ ).<sup>12</sup> For every added  $\text{Li}^+$ , one  $\text{Ni}^{2+}$  is promoted to the  $\text{Ni}^{3+}$  state, which is the lost

TABLE I. Lattice constant, grain size,  $\epsilon'$ , and activation energy for LTNO-1 and LTNO-2 samples.

Samples	Lattice parameter (Å)	Grain size ( $\mu\text{m}$ )	$\epsilon'$ (300 K and 1 kHz)	$E_a$ (eV)	$E_g$ (eV)	$E_{GB}$ (eV)
LTNO-1	4.173	$2.67 \pm 0.75$	5534	0.320	0.324	0.562
LTNO-2	4.175	$6.02 \pm 2.38$	11187	0.303	0.315	0.483



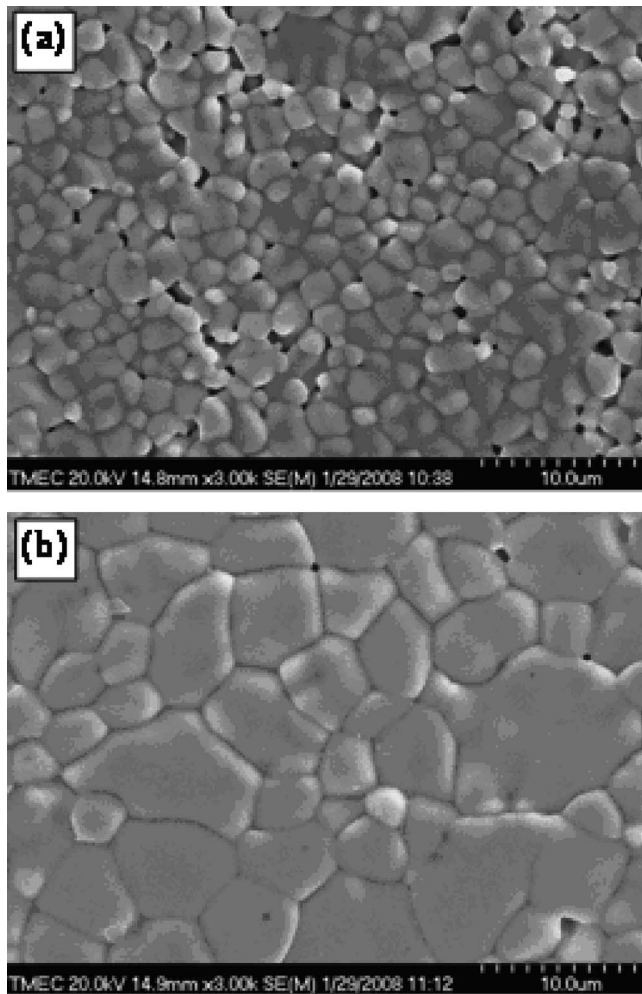


FIG. 2. SEM images of surface morphologies of (a) LTNO-1 and (b) LTNO-2.

electron filling a state in the oxygen  $2p$  valence band. The lattice now contains  $\text{Ni}^{2+}$  and  $\text{Ni}^{3+}$  ions on equivalent sites and is the model situation for conduction by polaron hopping.<sup>29</sup> In polaronic scenario, the temperature dependence of the conductivity is, with a temperature dependence prefactor, ascribed as,<sup>19</sup>

$$\sigma \propto T^{-1} \exp(-E/k_B T), \quad (1)$$

where  $E$ ,  $k_B$ , and  $T$  are the activation energy, Boltzmann constant, and absolute temperature, respectively. In general, the GB effect on electric conductivity may originate from a GB potential barrier, which should be ascribed by the Ti-rich boundary for (Li, Ti)-doped NiO system.<sup>19</sup> From the intercepts of each semicircular arc with the real axis, the resistance of the grain  $R_g$  and the resistance of the GB  $R_{GB}$  can be obtained. As a result, conductivity data were obtained for the grain ( $\sigma_g$ ) and GB ( $\sigma_{GB}$ ) components. We found from Fig. 3(b) that both  $\sigma_g$  and  $\sigma_{GB}$  values at different temperatures follow Eq. (1). Accordingly, in the LTNO-2 sample, the conduction activation energies inside the grain and at the GB were obtained to be  $E_g = 0.315$  eV and  $E_{GB} = 0.483$  eV, respectively. These results strongly indicate that the grain and GB have different characters of electrical transport, forming an electrically heterogeneous structure. This difference was

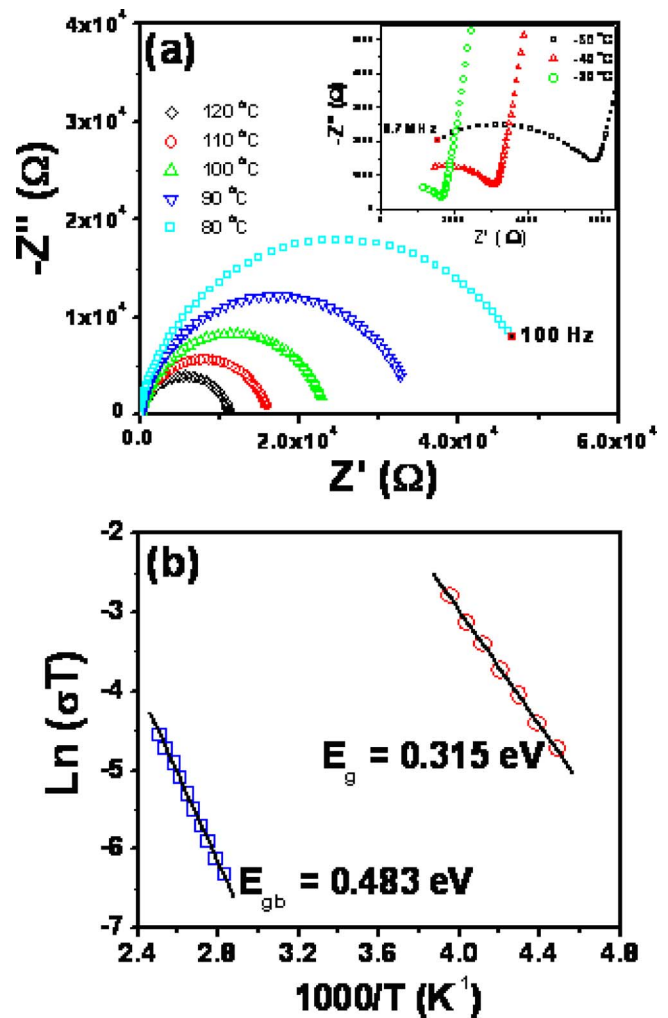


FIG. 3. (Color online) (a) Impedance spectra as a function of temperature for the LTNO-2 sample. Inset is the impedance spectra at low temperature. (b) The Arrhenius plots of the conductivities of the grain and the GB.

also observed in the LTNO-1 sample. The summary of activation energies and related parameters are also tabulated in Table I. From this point of view, it is appropriate to make the assumption that such the appearance of electrically heterogeneous should be a key factor of affecting the dielectric behavior in our LTNO ceramic samples.

To clarify the assumption above, we have studied the temperature dependence of  $\epsilon'$  and the dissipation factor ( $\tan \delta$ ) for LTNO samples at various frequencies, as shown in Fig. 4. It is clearly seen from Figs. 4(a) and 4(c) that both samples exhibit high- $\epsilon'$  of 5534 for LTNO-1 and 11 187 for LTNO-2 at room temperature and 1 kHz, and each sample has a similar dielectric behavior. Below 10 kHz, the dielectric constant is nearly temperature independent over the measured temperature range. However, with increasing frequency,  $\epsilon'$  dramatically drops to low values at low temperatures, being accompanied by the appearance of corresponding peaks in the  $\tan \delta$  [Figs. 4(b) and 4(d)]. Moreover, the  $\tan \delta$  peak moves to a higher temperature range with increasing frequency, which is a suggestion of the thermally excited relaxation process. With decreasing the temperature, the electric dipoles freeze through relaxation process and then the rate of polarization is decreased, resulting

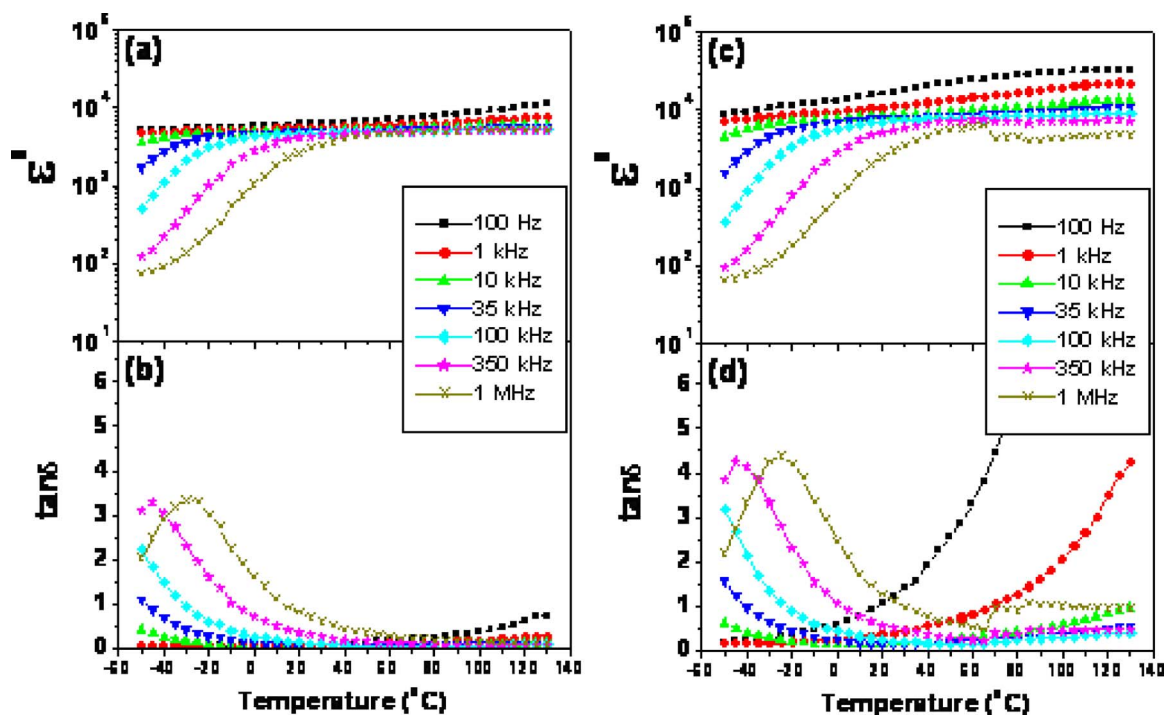


FIG. 4. (Color online) [(a) and (c)] Temperature dependence of  $\epsilon'$  for the LTNO-1 and LTNO-2, respectively. [(b) and (d)] Temperature dependence of  $\tan \delta$  for the LTNO-1 and LTNO-2, respectively.

in the dramatic decrease in  $\epsilon'$  value. According to the LTNO-2 sample, the increase in  $\tan \delta$  at high temperature is mainly due to the effect of dc conductivity.<sup>10</sup> Note that the overall dielectric behavior in the reported samples is similar to that observed in the other prepared LTNO methods,<sup>10,11</sup> which is in marked contrast to the well-known ferroelectric one, resulting from structure distortion due to a soft-mode

condensation. Therefore, the high dielectric response in our LTNO ceramics might be attributed to the apparent electrically heterogeneous structure in the ceramics.

We have further studied the frequency dependence of the real ( $\epsilon'$ ) part and imaginary part ( $\epsilon''$ ) of complex permittivity at various temperatures in order to obtain the underlying mechanism of high- $\epsilon'$  response in the LTNO samples, the

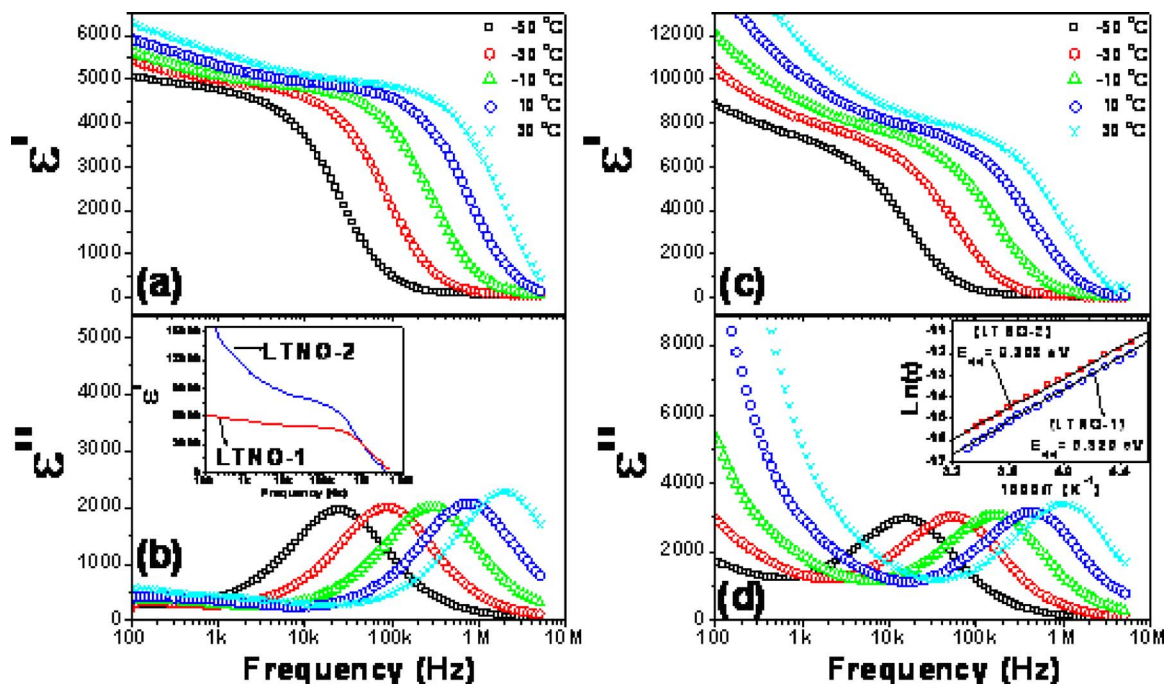


FIG. 5. (Color online) [(a) and (c)] Frequency dependence of  $\epsilon'$  for the LTNO-1 and LTNO-2, respectively. [(b) and (d)] Frequency dependence of  $\epsilon''$  for the LTNO-1 and LTNO-2, respectively. Inset of (b) shows the comparison of  $\epsilon'$  at room temperature over the measured frequencies. Inset of (d) demonstrates the Arrhenius plots of the relaxation process.

results are shown in Fig. 5. As demonstrated in Figs. 5(a) and 5(c), the  $\varepsilon'$  shows the high values at low frequencies, and it rapidly decreases if the frequency is sufficiently high. This step decrease shifts to higher frequency with increasing the temperature, corresponding to the movement of the  $\varepsilon''$  peaks. Such a behavior is typical for the Debye-like relaxation, which for the present work can be attributed to the MW relaxation. The MW relaxation model was usually employed to explain the observed high- $\varepsilon'$  in electrically inhomogeneous materials.<sup>19</sup> Thus, this may be the most appropriate one to elucidate the origin of high- $\varepsilon'$  in our LTNO samples due to the different electrical transport between the grain and the GB, as confirmed by the IS study (Fig. 3).

We now turn to see the dielectric relaxation behavior of the LTNO samples, which usually provide important clues for the explanation of the related mechanism.<sup>28</sup> The inset of Fig. 5(d) shows the plot of  $\ln(\tau)$  versus  $1/T$ , in which the solid line is the fitted result obeying the Arrhenius law, i.e.,

$$\tau = \tau_0 \exp(E_a/k_B T), \quad (2)$$

where  $\tau_0$  is the pre-exponential factor,  $E_a$  is the activation energy for the relaxation,  $k_B$  is the Boltzmann constant, and  $T$  is the absolute temperature.  $\tau$  is calculated from the relations  $\omega\tau=1$  and  $\omega=2\pi f_p$ , where  $\omega$  is angular frequency and  $f_p$  is the characteristic frequency corresponding to the peak of  $\varepsilon''$ , as displayed in Figs. 5(b) and 5(d). According to the fitted curve in the inset of Fig. 5(d), for the LTNO samples with different grain sizes, the activation energy ( $E_a$ ) for relaxation process can be obtained. The values of  $E_a$  are 0.320 and 0.303 eV for the samples of LTNO-1 and LTNO-2, respectively. From Table I, the activation energies of the conductivity in the grain interiors of the sample of LTNO-1,  $E_g \sim 0.324$  and LTNO-2,  $E_g \sim 0.315$  eV obtained from Fig. 3(b) are very close to the activation energies required for relaxations. These results imply that the nature of charge carriers responsible for dielectric relaxation peaks and dc conduction belongs to the same category, indicating that the polarization relaxation has a close relation to the conductivity in the grain interior.<sup>19</sup> Consequentially,  $E_a$  and  $E_g$  are almost the same in value and the polarization process depends on the conductivity of the charge inside the grain. This behavior is consistent with the literature report for LTNO prepared by sol-gel method.<sup>19</sup> According to the IS and dielectric results, here we think that the high- $\varepsilon'$  response in our LTNO ceramics is mainly due to the MW relaxation caused by the existent of electrically inhomogeneous in microstructure. Such structure is referred to as a core/shell structure, i.e., the LTNO samples consist of semiconducting grains enclosed by insulating boundaries, so the grains and their boundaries give rise to the different electrical response in the impedance formalism.

It is of interest to note that  $E_a$  decreases from 0.320 to 0.303 eV with increasing the grain size from  $2.67 \pm 0.75$  to  $6.02 \pm 2.38$   $\mu\text{m}$ , corresponding to the increase in  $\varepsilon'$ , as shown in Table I. As shown in the inset of Fig. 5(b),  $\varepsilon'$  value of LTNO-2 sample is higher than that of LTNO-1 sample over frequency range of 100 Hz–1 MHz. However,  $\varepsilon'$  of both samples is almost the same in value at the frequencies higher than 1 MHz. This is possibly due to the bulk effect.

Obviously,  $\varepsilon'$  increases with the sintering temperature and is accordingly closely related to the polycrystalline microstructure, particularly to the grain size. Thus, the differences in the values of  $\varepsilon'$  and  $E_a$  for the LTNO-1 and LTNO-2 samples are strongly affected by their microstructures. All these facts indicate that microstructures play a crucial role in changing the electrical properties and related dielectric behavior. The observed microstructure dependence of dielectric properties is similar to that observed in CCTO ceramics.<sup>27</sup>

According to the IS results, grain and GB in our LTNO samples have different values of conductivities ( $\sigma_g$  and  $\sigma_{GB}$ ) and dielectric permittivities ( $\varepsilon'_g$  and  $\varepsilon'_{GB}$ ). Therefore, the complex permittivity in the LTNO system can be described as<sup>30</sup>

$$\varepsilon_g^* = \varepsilon_g - j\sigma_g/\omega, \quad (3)$$

$$\varepsilon_{gb}^* = \varepsilon_{gb} - j\sigma_{gb}/\omega. \quad (4)$$

The total complex permittivity ( $\varepsilon^*$ ) can be quantitatively approximated by<sup>30</sup>

$$\varepsilon^* = L \left( \frac{t_g}{\varepsilon_g^*} + \frac{t_{gb}}{\varepsilon_{gb}^*} \right)^{-1}, \quad (5)$$

where  $t_g$  is the particle size of the conducting grain,  $t_{GB}$  is the thickness of boundary layer, and  $L = t_g + t_{GB}$ . Since  $L \gg t_{GB}$  and  $\sigma_g \gg \sigma_{GB}$ , Eq. (5) can be simplified as<sup>30</sup>

$$\varepsilon^* = \frac{\varepsilon_g}{a} + \left( \frac{\varepsilon_{gb}}{a\delta} \right) \left( \frac{1}{1 + j\omega\tau} \right), \quad (6)$$

where  $a = 1 + \delta\varepsilon_g/\varepsilon_{gb}$ ,  $\tau = a\varepsilon_{gb}/\delta\sigma_g$ , and  $\delta = t_{gb}/L$ .

At zero or very low frequency, the Eq. (6) can be further simplified as

$$\varepsilon' = \frac{L\varepsilon_{gb}}{t_{gb}}. \quad (7)$$

From the relation in Eq. (7), it is reasonable to propose that the different dielectric permittivity in LTNO-1 and LTNO-2 samples is affected by the grain size. Note that  $t_{GB}$  are about the same in value because it depends on the Ti-dopant concentration. It is important to note that the lower in dielectric permittivity in LTNO-1 sample may also be affected by the observed porosity, as shown in the SEM image of Fig. 2(a). However, we believe that the grain size is still the main effect on the dielectric properties of our LTNO ceramics. To support this conclusion, we consider the dielectric permittivity of LTNO-1 ( $\varepsilon_{\text{LTNO-1}} = 5534$ ) and LTNO-2 ( $\varepsilon_{\text{LTNO-2}} = 11187$ ) at room temperature and 1 kHz and evaluate the ratio of the dielectric permittivity of LTNO-2 and LTNO-1 based on the dimensions of the grain observed in SEM. Since both LTNO-1 and LTNO-2 have the same amount of Ti, the thickness of GB  $t_{GB}$  of these two samples may be assumed to be the same. From Eq. (7) and by assuming  $t_{GB}$  and  $\varepsilon_{GB}$  to be the same for both the LTNO-1 and LTNO-2, the ratio of the dielectric permittivity of LTNO-2 and LTNO-1 becomes



$$\frac{\varepsilon'_{\text{LTNO-2}}}{\varepsilon'_{\text{LTNO-1}}} = \frac{L_{\text{LTNO-2}}}{L_{\text{LTNO-1}}} \quad (8)$$

By substituting  $L_{\text{LTNO-1}} = 2.67 \pm 0.75 \mu\text{m}$  and  $L_{\text{LTNO-2}} = 6.02 \pm 2.38 \mu\text{m}$  into Eq. (8),  $\varepsilon'_{\text{LTNO-2}}/\varepsilon'_{\text{LTNO-1}}$  was obtained to be 2.25. This result agrees with the experimental result (i.e.,  $\varepsilon'_{\text{LTNO-2}}/\varepsilon'_{\text{LTNO-1}} = 11187/5534 = 2.02$ ).

For the present work, we speculate that high- $\varepsilon'$  response in the LTNO samples is attributed to their electrically inhomogeneous structures. When the alternative electric field is applied through the samples, the charge carriers are restricted by the Ti-rich boundary, and thus the opposite charges accumulate at the two edges of the GBs.<sup>19</sup> Consequentially, the polarization formation primarily depends on the accumulation of the charge via conducting in the grain interiors. This provides an extended description for the physical explanation for the underlying polarization. Therefore, the difference in  $\varepsilon'$  of LTNO samples with different grain size is attributed to the different amount of the accumulated charges at GBs. As well known, these accumulated charges in the LTNO ceramics depend on the concentration of monovalent impurities like  $\text{Li}^+$  ions.<sup>10</sup> For both of our samples, however, they have the same chemical composition, but different sintering temperature. Hence, the increase in  $\varepsilon'$  in the LTNO-2 sample with higher sintering temperature may be attributed to the other free charge carriers but does not related to the affect of the dopant concentration. One may deduce from this assumption that grains made by different sintering conditions could have very different electrical properties. The fact that the higher conduction activation energy of 0.324 eV for the grains in LTNO-1 sample than that of 0.315 eV for LTNO-2 sample may imply that there are lower oxygen vacancies concentration in the grains of LTNO-1 sample than in the grain of LTNO-2 sample. This is reasonable because the LTNO-2 sample was fabricated at the temperature of 1280 °C, which is higher than that of 1200 °C for the LTNO-1. Based on the explanation above, we think that the oxygen vacancies have the influence on the electrical properties of the LTNO ceramics and the contribution to the total dielectric response in a LTNO system. However, the evidence of the presence of oxygen vacancies is beyond the scope of our work, and further work, i.e., the study of heat treatment effects on the oxidizing and/or reducing atmosphere on electrical properties, is needed to make a more detailed explanation for it. It is worth to noting that the lower  $\tau_0$  values of the LTNO-1 sample than those of the LTNO-2 sample over the measured temperature is attributed to the shorter distance between the nearest GBs in the LTNO-1 sample compared to the larger grain for the LTNO-2 sample. Thus, the polarization of LTNO-1 sample is fully developed at higher frequency than that of LTNO-2 sample at the same temperature as shown in Fig. 5. This result was also observed in CCTO ceramics.<sup>31</sup> Additionally,  $E_{\text{GB}}$  also decreases with increasing the sintering temperature (Table I). This is associated to the ceramic microstructure of LTNO samples. We think that the higher  $E_{\text{GB}}$  observed in the LTNO-1 sample compared to that of the LTNO-2 sample is attributed to the observed porosity in the LTNO-1 sample. Some of the GB regions are replaced by the porosities (air gaps) in the

LTNO-1 ceramic, and thus the total potential barrier at the GB regions increases. Another possible of such observation is that the defect equilibrium at the GB regions may be modified by the increase of grain size, affecting on the electrical transport at the regions.

#### IV. CONCLUSION

The high- $\varepsilon'$  of LTNO ceramics have been synthesized by a simple thermal decomposition method. The complex impedance spectroscopy indicates that the electrically heterogeneous structures exist in the LTNO ceramics consisting of semiconducting grain and insulating GB. The  $\varepsilon'$  value of our LTNO ceramics increases with the increase in grain size, and the dielectric response can be well explained by the MW relaxation model. The experimental results indicate that the polarization relaxation has a close relation to the conductivity inside the grain. Our results also reveal that  $E_a$  and related  $E_g$  and  $E_{\text{GB}}$  decrease with the increase in grain size. It can be proposed that the different microstructures lead to the chemical change (e.g., oxygen vacancies) inside the grains and at the GBs.

#### ACKNOWLEDGMENTS

The authors would like to thank the Department of Physics, Ubon Ratchathani University for providing XRD facilities, and the Thai Microelectronics Center (TMEC) for FE-SEM facilities. P.T. would like to thank the Thailand Graduate Institute of Science and Technology (TGIST) for his PhD scholarship. This work is financially supported by The Thailand Research Fund (TRF) and The Higher Commission Education (HCE), The Ministry of Education, Thailand.

- <sup>1</sup>C. C. Homes, T. Vogt, S. M. Shapiro, S. Wakimoto, and A. P. Ramirez, *Science* **293**, 673 (2001).
- <sup>2</sup>M. A. Subramanian, D. Li, N. Duan, B. A. Reisner, and A. W. Sleight, *J. Solid State Chem.* **151**, 323 (2000).
- <sup>3</sup>A. P. Ramirez, M. A. Subramanian, M. Gardel, G. Blumberg, D. Li, T. Vogt, and S. M. Shapiro, *Solid State Commun.* **115**, 217 (2000).
- <sup>4</sup>C. Masingboon, S. Maensiri, T. Yamwong, P. L. Anderson, and S. Seraphin, *Appl. Phys. A: Mater. Sci. Process.* **91**, 87 (2008).
- <sup>5</sup>S. F. Shao, J. L. Zhang, P. Zheng, and C. L. Wang, *Solid State Commun.* **142**, 281 (2007).
- <sup>6</sup>D. C. Sinclair, T. B. Adams, F. D. Morrison, and A. R. West, *Appl. Phys. Lett.* **80**, 2153 (2002).
- <sup>7</sup>C. Masingboon, P. Thongbai, S. Maensiri, T. Yamwong, and S. Seraphin, *Mater. Chem. Phys.* **109**, 262 (2008).
- <sup>8</sup>S. Maensiri, P. Thongbai, and T. Yamwong, *Appl. Phys. Lett.* **90**, 202908 (2007).
- <sup>9</sup>P. Lunkenheimer, R. Fichtl, S. G. Ebbinghaus, and A. Loidl, *Phys. Rev. B* **70**, 172102 (2004).
- <sup>10</sup>J. Wu, C. W. Nan, Y. Lin, and Y. Deng, *Phys. Rev. Lett.* **89**, 217601 (2002).
- <sup>11</sup>S. Maensiri, P. Thongbai, and T. Yamwong, *Acta Mater.* **55**, 2851 (2007).
- <sup>12</sup>Y. Lin, J. Wang, L. Jiang, Y. Chen, and C. W. Nan, *Appl. Phys. Lett.* **85**, 5664 (2004).
- <sup>13</sup>Y. Lin, L. Jiang, R. Zhao, and C. W. Nan, *Phys. Rev. B* **72**, 014103 (2005).
- <sup>14</sup>P. K. Jana, S. Sarkar, and B. K. Chaudhuri, *Appl. Phys. Lett.* **88**, 182901 (2006).
- <sup>15</sup>P. K. Jana, S. Sarkar, H. Sakata, T. Watanabe, and B. K. Chaudhuri, *J. Phys. D* **41**, 065403 (2008).
- <sup>16</sup>Y. J. Hsiao, Y. S. Change, T. H. Fang, T. L. Chai, C. Y. Chung, and Y. H. Chang, *J. Phys. D* **40**, 863 (2007).
- <sup>17</sup>S. Sarkar, P. K. Jana, B. K. Chaudhuri, and H. Sakata, *Appl. Phys. Lett.* **89**, 212905 (2006).

- <sup>18</sup>P. Thongbai, S. Maensiri, and T. Yamwong, *J. Appl. Phys.* **104**, 036107 (2008).
- <sup>19</sup>Y. H. Lin, M. Li, C. W. Nan, J. Li, J. Wu, and J. He, *Appl. Phys. Lett.* **89**, 032907 (2006).
- <sup>20</sup>Y. Lin, R. Zhao, J. Wang, J. Cai, C. W. Nan, Y. Wang, and L. Wei, *J. Am. Ceram. Soc.* **88**, 1808 (2005).
- <sup>21</sup>T. B. Adams, D. C. Sinclair, and A. R. West, *J. Am. Ceram. Soc.* **89**, 3129 (2006).
- <sup>22</sup>B. A. Bender and M.-J. Pan, *Mater. Sci. Eng., B* **117**, 339 (2005).
- <sup>23</sup>P. Thongbai, C. Masingboonl, S. Maensiri, T. Yamwong, S. Wongsanmai, and R. Yimnirun, *J. Phys.: Condens. Matter* **19**, 236208 (2007).
- <sup>24</sup>P. Thongbai, S. Maensiri, T. Yamwong, and R. Yimnirun, *J. Appl. Phys.* **103**, 114107 (2008).
- <sup>25</sup>T.-T. Fang and C. P. Liu, *Chem. Mater.* **17**, 5167 (2005).
- <sup>26</sup>T. B. Adams, D. C. Sinclair, and A. R. West, *Adv. Mater. (Weinheim, Ger.)* **14**, 1321 (2002).
- <sup>27</sup>S. F. Shao, J. L. Zhang, P. Zheng, W. L. Zhong, and C. L. Wang, *J. Appl. Phys.* **99**, 084106 (2006).
- <sup>28</sup>J. R. Macdonald, *Impedance Spectroscopy* (Wiley, New York, 1987).
- <sup>29</sup>A. J. Moulson and J. M. Herbert, *Electroceramics* (Wiley, New York, 2003).
- <sup>30</sup>I. P. Raevski, S. A. Prosandeev, A. S. Bogatin, M. A. Malitskaya, and L. Jastrabik, *J. Appl. Phys.* **93**, 4130 (2003).
- <sup>31</sup>W. Li and R. W. Schwartz, *Appl. Phys. Lett.* **89**, 242906 (2006).
- <sup>32</sup>JCPDS Card No. 78-0429.